3.5 Discussion

3.5.1 Upregulation of Autophagy in CNS Injury

Previous studies demonstrated the expression of Beclin 1 to increase at lesion sites after traumatic brain injury and cerebral ischemia [9, 18, 31]. In such diseases, expression of LC3 increases at the lesion sites [18, 32–35]. These reports suggest that the autophagic activity increases in response to the neural tissue damage of the brain. Our previous studies first reported the increased expression of Beclin 1 and LC3 in the damaged neural tissue after SCI [25, 26]. Using electron microscopy, we also confirmed that the formation of autophagic vacuoles also increased in the damaged cells of the injured spinal cord [26]. Therefore, autophagy was activated in the damaged neural tissue after SCI.

3.5.2 Neuroprotective Function of Autophagy

Many studies reported that autophagy has a cytoprotective function against cell death. Autophagy has a cytoprotective function in neurodegenerative diseases [10–13]. Autophagy induced neuroprotection in traumatic brain injury and in neonatal hypoxia-ischemia induced brain injury [9, 36]. In models of Huntington disease, the stimulation of autophagy protects cells against apoptosis [37]. In addition, the inhibition of autophagy increases the apoptosis of neurons and also causes neurodegeneration in mice [10, 11]. One potential mechanism underlying these neuroprotective effects is the blocking of apoptosis by the activation of autophagy [12, 36, 38]. Interestingly, it has been suggested that mTOR inhibition enhances the clearance of mitochondria by inducing autophagy, thereby reducing cytosolic cytochrome c release and downstream caspase activation [24, 39]. Previous studies have demonstrated that inhibition of mTOR upregulates autophagy and shows cytoprotective functions by reducing apoptosis in various disease models, including the myocardial ischemia-reperfusion model [38] and neonatal hypoxia-ischemia-induced brain injury model [36]. In our results, rapamycin promoted autophagy by inhibiting the mTOR signaling and reduced neural tissue damage such as neuronal loss and cell death following SCI. These results suggested autophagy produced neuroprotective effect after SCI.

3.5.3 Autophagy Modulation as a Therapeutic Target for SCI

Autophagy may be dysregulated in various disorders, including metabolic diseases, neurodegenerative disorders, infectious diseases, and cancer. In several conditions, autophagy is inhibited and this can occur at different stages of the process to enhance disease, whereas in other cases autophagic activity may be permissive towards

pathogenesis [24]. Recently, pharmacological approaches to upregulate or inhibit autophagy are receiving considerable attention. For example, autophagy upregulation may be of therapeutic benefit in certain neurodegenerative diseases and trauma [9, 36, 39]. Indeed, our study demonstrated that upregulation autophagy by mTOR inhibitor, rapamycin, resulted in reduction of neural tissue damage and locomotor impairment after SCI [28]. Therefore, the pharmacological modulation of autophagy may have clinical benefits for treatment of patients with SCI. Further studies to clarify the neuroprotective and neuroregenerative mechanisms regulated by autophagy are needed in order to approve the clinical use of pharmacological modulation of autophagy for patients with acute SCI.

3.5.4 Autophagic Cell Death

The autophagic process can lead to nonapoptotic programmed cell death, which is known as autophagic cell death [8]. Autophagic cell death is morphologically distinct from necrotic cell death and apoptotic cell death [14, 16]. The nucleus is shrunken and fragmented in apoptosis, but in autophagic cell death, the nucleus does not change [14, 18, 31]. Previous studies have shown autophagic cell death to be induced after brain trauma and cerebral ischemia and contributed to neural tissue damage [31, 33]. Our studies demonstrated that most of the nuclei in the TUNEL-positive cells expressed Beclin 1 or LC3 were round, which should normally be observed in autophagic cell death, and they were not either shrunken or fragmented as is observed in apoptotic nuclei [26, 40]. Therefore, these findings suggested autophagic cell death may occur in the injured spinal cord. However, the molecular mechanism defining the features of autophagic cell death is still unknown [8, 41, 42]. Further studies are needed to clarify the molecular mechanism of autophagic cell death in SCI.

3.6 Conclusion

Our previous studies demonstrated that molecular markers of autophagy such as Beclin 1 and LC3 were significantly upregulated in the injured spinal cord. The increased activity of autophagy was observed in neurons, astrocytes, and oligodendrocytes at the lesion site. Electron microscopy showed an increased formation of autophagic vacuoles in the damaged neural cells. In addition, the rapamycin administration in acute phase of SCI promoted autophagy in the injured spinal cord and reduced neural tissue damage and locomotor impairment. These findings indicated that autophagic activity is increased in damaged neural tissue after SCI. Furthermore the promotion of autophagy by rapamycin treatment can provide neuroprotective effect to improve locomotor function following SCI.

Conflict of Interest The authors declare that they have no conflict of interest.

References

1. Gozuacik D, Kimchi A (2004) Autophagy as a cell death and tumor suppressor mechanism. Oncogene 23:2891–2906
2. Klionsky D, Emr S (2000) Autophagy as a regulated pathway of cellular degradation. Science 290:1717–1721
3. Larsen K, Sulzer D (2002) Autophagy in neurons: a review. Histol Histopathol 17:897–908
4. Ogier-Denis E, Codogno P (2003) Autophagy: a barrier or an adaptive response to cancer. Biochim Biophys Acta 1603:113–128
5. Levine B, Klionsky D (2004) Development by self-digestion: molecular mechanisms and biological functions of autophagy. Dev Cell 6:463–477
6. Mele´ndez A, Tallo´czy Z, Seaman M et al (2003) Autophagy genes are essential for dauer development and life-span extension in *C. elegans*. Science 301:1387–1391
7. Rubinsztein DC, DiFiglia M, Heintz N et al (2005) Autophagy and its possible roles in nervous system diseases, damage and repair. Autophagy 1(1):11–22. doi:1513[pii]
8. Tsujimoto Y, Shimizu S (2005) Another way to die: autophagic programmed cell death. Cell Death Differ 12(Suppl 2):1528–1534. doi:10.1038/sj.cdd.4401777
9. Erlich S, Alexandrovich A, Shohami E et al (2007) Rapamycin is a neuroprotective treatment for traumatic brain injury. Neurobiol Dis 26:86–93
10. Hara T, Nakamura K, Matsui M et al (2006) Suppression of basal autophagy in neural cells causes neurodegenerative disease in mice. Nature 441(7095):885–889. doi:nature04724 [pii], 10.1038/nature04724
11. Komatsu M, Waguri S, Chiba T et al (2006) Loss of autophagy in the central nervous system causes neurodegeneration in mice. Nature 441(7095):880–884. doi:10.1038/nature04723
12. Pan T, Kondo S, Zhu W et al (2008) Neuroprotection of rapamycin in lactacystin-induced neurodegeneration via autophagy enhancement. Neurobiol Dis 32:16–25
13. Sarkar S, Ravikumar B, Floto RA et al (2009) Rapamycin and mTOR-independent autophagy inducers ameliorate toxicity of polyglutamine-expanded huntingtin and related proteinopathies. Cell Death Differ 16(1):46–56. doi:10.1038/cdd.2008.110
14. Kitanaka C, Kuchino Y (1999) Caspase-independent programmed cell death with necrotic morphology. Cell Death Differ 6(6):508–515. doi:10.1038/sj.cdd.4400526
15. Scarlatti F, Granata R, Meijer AJ et al (2009) Does autophagy have a license to kill mammalian cells? Cell Death Differ 16(1):12–20. doi:cdd2008101 [pii], 10.1038/cdd.2008.101
16. Clarke PG (1990) Developmental cell death: morphological diversity and multiple mechanisms. Anat Embryol 181(3):195–213
17. Matsui Y, Takagi H, Qu X et al (2007) Distinct roles of autophagy in the heart during ischemia and reperfusion: roles of AMP-activated protein kinase and Beclin 1 in mediating autophagy. Circ Res 100(6):914–922. doi:10.1161/01.RES.0000261924.76669.36
18. Rami A, Langhagen A, Steiger S (2008) Focal cerebral ischemia induces upregulation of Beclin 1 and autophagy-like cell death. Neurobiol Dis 29:132–141
19. Suzuki C, Isaka Y, Takabatake Y et al (2008) Participation of autophagy in renal ischemia/reperfusion injury. Biochem Biophys Res Commun 368(1):100–106. doi:10.1016/j.bbrc.2008.01.059
20. Liang XH, Jackson S, Seaman M et al (1999) Induction of autophagy and inhibition of tumorigenesis by Beclin 1. Nature 402(6762):672–676. doi:10.1038/45257
21. Kihara A, Kabeya Y, Ohsumi Y et al (2001) Beclin-phosphatidylinositol 3-kinase complex functions at the trans-Golgi network. EMBO Rep 2(4):330–335. doi:10.1093/embo-reports/kve061
22. Mizushima N (2004) Methods for monitoring autophagy. Int J Biochem Cell Biol 36:2491–2502
23. Kabeya Y, Mizushima N, Ueno T et al (2000) LC3, a mammalian homologue of yeast Apg8p, is localized in autophagosome membranes after processing. EMBO J 19:5720–5728
24. Rubinsztein DC, Codogno P, Levine B (2012) Autophagy modulation as a potential therapeutic target for diverse diseases. Nat Rev Drug Discov 11(9):709–730. doi:10.1038/nrd3802

25. Kanno H, Ozawa H, Sekiguchi A et al (2009) Spinal cord injury induces upregulation of Beclin 1 and promotes autophagic cell death. Neurobiol Dis 33:143–148
26. Kanno H, Ozawa H, Sekiguchi A et al (2011) Induction of autophagy and autophagic cell death in damaged neural tissue after acute spinal cord injury in mice. Spine (Phila Pa 1976) 36(22):E1427–E1434. doi:10.1097/BRS.0b013e3182028c3a
27. Kanno H, Ozawa H, Sekiguchi A et al (2009) The role of autophagy in spinal cord injury. Autophagy 5(3):390–392. doi:7724 [pii]
28. Sekiguchi A, Kanno H, Ozawa H et al (2012) Rapamycin promotes autophagy and reduces neural tissue damage and locomotor impairment after spinal cord injury in mice. J Neurotrauma 29(5):946–956. doi:10.1089/neu.2011.1919
29. Kanno H, Ozawa H, Sekiguchi A et al (2012) The role of mTOR signaling pathway in spinal cord injury. Cell Cycle 11(17):3175–3179. doi:10.4161/cc.21262
30. Basso DM, Fisher LC, Anderson AJ et al (2006) Basso Mouse Scale for locomotion detects differences in recovery after spinal cord injury in five common mouse strains. J Neurotrauma 23(5):635–659. doi:10.1089/neu.2006.23.635
31. Diskin T, Tal-Or P, Erlich S et al (2005) Closed head injury induces upregulation of Beclin 1 at the cortical site of injury. J Neurotrauma 22:750–762
32. Liu CL, Chen S, Dietrich D et al (2008) Changes in autophagy after traumatic brain injury. J Cereb Blood Flow Metab (Official J Int Soc Cereb Blood Flow Metab) 28(4):674–683. doi:10.1038/sj.jcbfm.9600587
33. Adhami F, Liao G, Morozov YM et al (2006) Cerebral ischemia-hypoxia induces intravascular coagulation and autophagy. Am J Pathol 169(2):566–583. doi:10.2353/ajpath.2006.051066
34. Uchiyama Y, Koike M, Shibata M (2008) Autophagic neuron death in neonatal brain ischemia/hypoxia. Autophagy 4(4):404–408
35. Wen YD, Sheng R, Zhang LS et al (2008) Neuronal injury in rat model of permanent focal cerebral ischemia is associated with activation of autophagic and lysosomal pathways. Autophagy 4(6):762–769
36. Carloni S, Buonocore G, Balduini W (2008) Protective role of autophagy in neonatal hypoxia-ischemia induced brain injury. Neurobiol Dis 32:329–339
37. Ravikumar B, Vacher C, Berger Z et al (2004) Inhibition of mTOR induces autophagy and reduces toxicity of polyglutamine expansions in fly and mouse models of Huntington disease. Nat Genet 36:585–595
38. Khan S, Salloum F, Das A et al (2006) Rapamycin confers preconditioning-like protection against ischemia-reperfusion injury in isolated mouse heart and cardiomyocytes. J Mol Cell Cardiol 41:256–264
39. Ravikumar B, Berger Z, Vacher C et al (2006) Rapamycin pre-treatment protects against apoptosis. Hum Mol Genet 15:1209–1216
40. Kanno H, Ozawa H, Sekiguchi A et al (2009) Spinal cord injury induces upregulation of Beclin 1 and promotes autophagic cell death. Neurobiol Dis 33(2):143–148. doi:S0969-9961(08)00217-9 [pii], 10.1016/j.nbd.2008.09.009
41. Kroemer G, Levine B (2008) Autophagic cell death: the story of a misnomer. Nat Rev Mol Cell Biol 9(12):1004–1010. doi:10.1038/nrm2529
42. Galluzzi L, Vitale I, Abrams JM et al (2012) Molecular definitions of cell death subroutines: recommendations of the Nomenclature Committee on Cell Death 2012. Cell Death Differ 19(1):107–120. doi:10.1038/cdd.2011.96

Chapter 6
Biomechanics of the Spinal Cord and the Pia Mater

Hiroshi Ozawa, Takeo Matsumoto, Toshiro Ohashi, and Masaaki Sato

Abstract Biomechanical analysis of the spinal cord is important to clarify the morphological plasticity of the spinal cord. In the present study, the elastic moduli of the gray and white matter were measured in situ by using a pipette aspiration method. The mechanical properties and function of the pia mater were investigated. Furthermore, the effect of the tensile stress on the morphology of the spinal cord was investigated. No significant difference in elastic moduli was observed between the gray and white matter of spinal cord. The elastic modulus of the pia mater was 2,300 kPa, which was 460 times higher than that of the spinal cord parenchyma. The pia mater triples the elastic modulus of the spinal cord covered by it compared with the parenchyma and increases the overall stiffness of the spinal cord. As a result of being tightly covered by the pia mater, the compressed spinal cord contains a large amount of strain energy, which enables shape restoration after decompression. The length of the spinal cord was decreased by 9.7 % after the separation to remove longitudinal tensile stress. The tensile stress along the craniocaudal axis in the spinal cord did not affect the spinal cord deformation in response to the compression, but it did affect the shape recoverability after the decompression.

Keywords Biomechanics • Elastic modulus • Pia mater • Spinal cord

H. Ozawa (✉)
Department of Orthopaedic Surgery, Tohoku University School of Medicine,
1-1 Seiryomachi, Aobaku, Sendai 980-8574, Japan
e-mail: hozawa@med.tohoku.ac.jp

T. Matsumoto
Department of Mechanical Engineering, Nagoya Institute of Technology, Nagoya, Japan

T. Ohashi
Faculty of Engineering, Hokkaido University, Sapporo, Japan

M. Sato
Graduate School of Biomedical Engineering, Tohoku University, Sendai 980-8574, Japan

K. Uchida et al. (eds.), *Neuroprotection and Regeneration of the Spinal Cord*,
DOI 10.1007/978-4-431-54502-6_6, © Springer Japan 2014

6.1 Introduction

Biomechanical analysis of the spinal cord is important to clarify the morphological plasticity of the spinal cord. The spinal cord is deformed in response to compression, and as a result, its cross-sectional area is reduced as observed on CT myelograms and axial MR images obtained in patients with cervical compressive myelopathy. Several factors regulate the deformation of the spinal cord. The elastic modulus of the parenchyma and the Poisson ratio are physical factors inherent in the spinal cord. The pia mater and the dentate ligament are factors that may affect the physical attributes of the spinal cord. The spinal cord is physiologically stretched along the craniocaudal axis and is subjected to tensile stress.

In the present study, the elastic moduli of the gray and white matter were measured in situ by using a pipette aspiration method. The mechanical properties and function of the pia mater were investigated. Furthermore, the effect of the tensile stress on the morphology of the spinal cord was investigated.

6.2 Elastic Moduli of the Gray and White Matter of the Spinal Cord

The gray matter of the spinal cord mainly consists of nerve cells, whereas the white matter consists of dendrites and axons. The gray matter has been thought to be softer than the white matter [1, 2], although no definite evidence to this effect has been published. In the present study, the elastic moduli of the gray and white matter were measured in situ by using a pipette aspiration method, which we have developed for the assessment of soft biological tissue.

6.2.1 Materials and Methods

6.2.1.1 Specimen Preparation

Eight Japanese white rabbits weighing an average of 2,600 g (range 2,400–2,800 g) were killed by intravenous injection of a high dose of pentobarbiturate. The C4–6 spinal column containing the spinal cord was excised from each rabbit. Using an osteotome, each column was transversely cut at the level of the intervertebral discs. Three spinal cord specimens were removed from their respective vertebral canals, and they were immediately placed in physiological saline at room temperature (16 °C) until mechanical testing.

Each of the three-dimensional cross sections (axial, frontal, and sagittal) was displayed as follows by using a microslicer: a specimen was cut transversely for the axial section; the second specimen from the same rabbit was vertically cut anterior

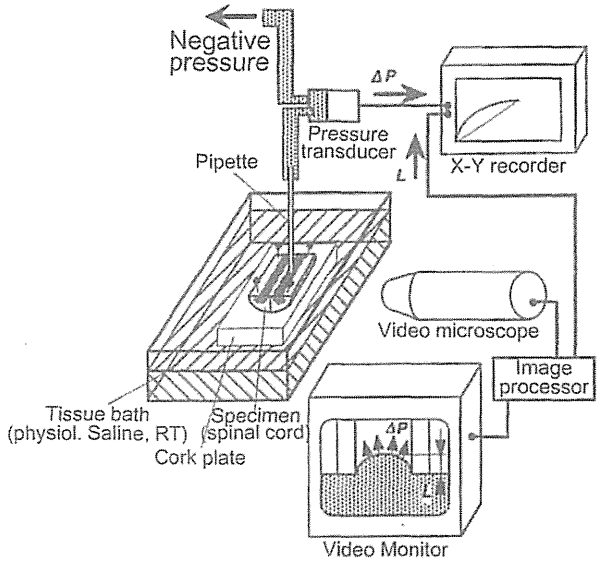

Fig. 6.1 Schematic diagram of the experimental setup

to the central canal for the frontal section; and the last specimen was cut in the middle of the right half of the spinal cord for the sagittal section. The gray and white matter were distinguished by their colors on the surface of each cross section.

The specimens were treated carefully and quickly so that testing was completed within 15 min after cutting with the microslicer. As long as each specimen was only visually inspected, the surface of the specimens did not begin dissolving into the physiological saline within 30 min after the cutting. All experiments were finished within 1 h after the rabbit was killed.

6.2.1.2 Experimental Apparatus and Procedure

The experimental setup used in the present study was similar to that used by Ohashi et al. [2] except for the apparatus used to apply negative pressure to the specimens (Fig. 6.1). As a substitute, we used a small vacuum pump with a large reservoir (20 L) to control the negative pressure precisely.

Each specimen was fixed on a cork plate by pins with the cut surface to be measured facing upward. Care was taken not to apply any external load. A glass pipette (0.8 mm in inner and 1.09 mm in outer diameter) was connected to a reservoir and a pressure transducer with silicone tubing. All of the tubing was filled with physiological saline. The transducer was calibrated with a mercury manometer before each experiment. The color was noticeably different between the white and gray matter on the cut surface. After a micromanipulator was used to set the tip of the pipette perpendicular to the gray or white matter appearing on the cut surface of the specimen, negative pressure was applied at a rate of -1 cm H_2O/s (range 0 to -5 cm H_2O).

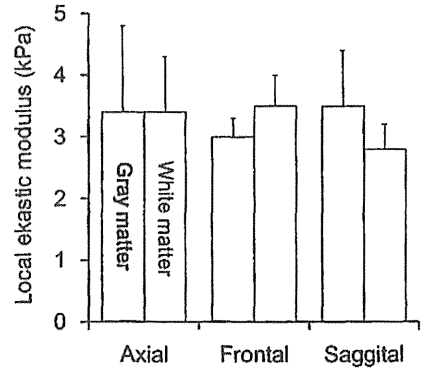

Fig. 6.2 Elastic moduli of *gray* and *white* matter of the spinal cord ($n=8$, mean±SD). The difference between the *gray* and *white* matter was significant neither in each section nor among all cross sections

To measure the elastic moduli of the gray and white matter separately, the pipette was applied to areas at least 1 mm apart from the boundary between the two types of matter. The deformation process of the aspirated tissue into the pipette was observed on a video monitor through a video microscope. The aspirated length was measured with a video dimension analyzer, and the pressure–deformation curve was continuously recorded on an X–Y recorder.

6.2.1.3 Determination of Local Modulus of Elasticity

In a separate study [3], finite element analysis of the pipette aspiration method was performed. The initial value of the modulus of elasticity (i.e., the Young modulus) was calculated by comparing the pressure–deformation curve obtained in the experiment with that in the finite element analysis.

6.2.2 Results

The pressure–deformation curves revealed typical hysteresis. Accordingly, the pressure–deformation relationship during aspiration was different from that during unloading, indicating that the spinal cord has marked viscoelasticity.

The elastic moduli of the gray and white matter were 3.4±1.4 (mean±SD) and 3.4±0.9 kPa in the axial section, 3.0±0.3 and 3.5±0.5 kPa in the frontal section, and 3.5±0.9 and 2.8±0.4 kPa in the sagittal section, respectively. The difference between the elastic moduli of the gray and white matter was significant neither in each section nor among all sections using the Kruskal–Wallis test (Fig. 6.2).

6.2.3 Discussion

The pipette aspiration technique was originally applied to the measurement of the mechanical properties of red cells and endothelial cell membranes of vessels [4]. By changing the diameter of the pipette, any size of soft tissue can be tested [5]. One of the advantages of this method is that different areas in a specimen can be measured in situ. The computer simulation has indicated that the modulus of elasticity obtained by this method is an averaged one of the hemispheric area with the diameter corresponding to the pipette diameter at its tip [3]. When using this method, the prerequisite condition of specimens is that they are soft enough to deform under the aspiration pressure applied through the pipette. In the present study, by using a thin pipette of 0.8 mm in diameter, the elastic moduli of the gray and the white matter could be measured separately in situ.

One of the limitations of this study is that we had to cut specimens to display the surface to be aspirated. Because nerve cells connect with their axons and dendrites in the gray matter and dendrites and axons adhere to each other in the white matter, cutting of the specimen would break such connections, and the tissue adjacent to the cut surface may become loose. The Young modulus measured on the surface of the gray and white matter may thus be a little lower than that measured in vivo. Nevertheless, at present there is no experimental evidence to refute the absence of significant difference in elastic moduli found between the gray and white matter in the present study.

6.3 Mechanical Properties and Function of the Spinal Pia Mater

Little attention has been paid to the function of the pia mater. In current accounts the function of the pia mater is described as that of a scaffold for the vasculature of the spinal cord parenchyma such as the anterior and posterior spinal arteries [6, 7]. There have been several articles concerning the mechanical properties of the pia mater [8, 9]; although its elasticity has been described, the elastic modulus of the pia mater has not been measured.

In the present study, the mechanical properties and function of the pia mater were investigated using the following methods: (1) a tensile test of the rabbit spinal cord with and without the pia mater to measure its elastic modulus and (2) a compression test of the rabbit spinal cord to clarify the effect of the pia mater on spinal cord stiffness.

6.3.1 Measurement of the Elastic Modulus of the Pia Mater

6.3.1.1 Specimen Preparation

Nine Japanese white rabbits were killed by intravenous injection of a high dose of pentobarbital. The cervical spinal column and cord from C5 through C6 were excised from each rabbit. Spinal cord segments were removed from the excised

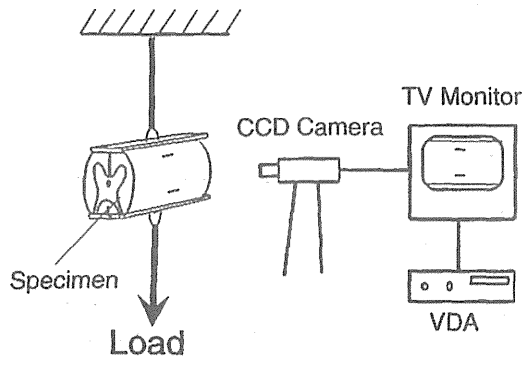

Fig. 6.3 Tensile test of the spinal cord. A specimen was hung up with the ventral plate and slightly elongated with a small load hooked on the dorsal plate. The image of the specimen was continuously taken with a CCD camera and displayed on a TV monitor. The load was increased at 60 s intervals, and the vertical distance between two predetermined marks on the specimen surface was measured

spinal columns taking care to keep the pia mater intact. The specimens were immediately placed in a physiological saline solution at room temperature (16 °C) until mechanical testing. All tests were accomplished within 30 min after the excision.

6.3.1.2 Tensile Test

For the tensile test, each spinal cord segment was cut into two pieces whose axial lengths were about 10 mm. One was the piece with the pia mater, and the other was the one whose pia mater had been carefully stripped off circumferentially under a microscope. Two small plastic plates (3 × 10 mm), each with a hook, were attached to the ventral and dorsal sides of the specimen with cyanoacrylate adhesive. Each specimen was then hung up with the hook of the ventral plate and was slightly elongated with a small load (0.32 g) on the dorsal plate. The image of the specimen was taken continuously with a CCD camera [OVM1000NM, Olympus, Japan] and displayed on a TV monitor (Fig. 6.3). The axial length (*lo*) and width (*wo*) of the specimen and vertical distance (*do*) between two predetermined marks on the specimen surface were measured on the TV monitor at the initial load. The load (F) was increased with 1.23 g (specimens with pia) or 0.49 g (specimens without pia), each at 60 s intervals, and the vertical distance between the marks (d) was measured at each loading immediately before the increment.

6.3.1.3 Calculation of the Elastic Modulus of the Pia Mater

The load–elongation (F–d) relationship of each specimen was converted into the stress–strain relationship using *lo*, *wo*, and *do*. Strain (λ) was calculated as the form of the stretch ratio:

$$\lambda = d / do.$$

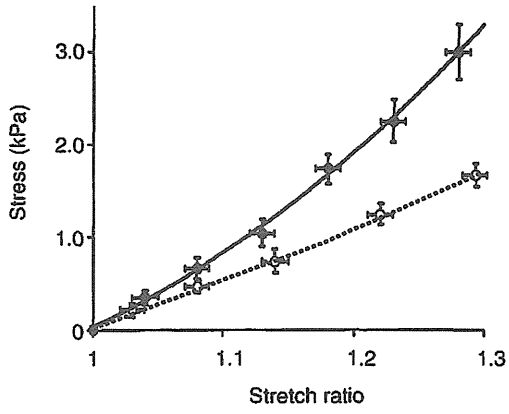

Fig. 6.4 Stress–strain curve was linear in the spinal cord without the pia mater. In contrast, the stress–strain relationship was nonlinear in the spinal cord with the pia mater, showing a concave upward curve that is commonly observed in connective tissue (*open circle*, spinal cord without pia; *filled circle*, spinal cord with pia; mean ± SEM)

Stress (σ) was obtained assuming incompressibility as follows:

$$\sigma = F\lambda / (wo\,lo).$$

Elastic moduli of specimens with the pia mater (*Eall*) and those of specimens without the pia mater (*Emed*) were obtained from the slope of the stress–strain curve. The mean thickness of the pia mater (*wpia*) was measured in histological sections of intact spinal cords.

The spinal cord parenchyma and pia mater were regarded as a composite material of the Voigt model. The elastic modulus of the composite material is a summation of the values of multiplication of the elastic moduli and volume ratio of each material. In other words, the elastic modulus of the whole spinal cord including the pia mater (*Eall*) depends on the elastic moduli of the pia mater and the spinal cord parenchyma and the ratio of their thickness. The apparent elastic modulus (*Eall*) can be expressed as follows according to the rule of mixtures:

$$Eall = Epia \cdot 2wpia / wo + Emed(1 - 2wpia / wo).$$

The elastic modulus of the pia mater (*Epia*), therefore, is given by the following equation:

$$Epia = \{Eall \cdot wo - Emed(wo - 2wpia)\} / (2wpia).$$

6.3.1.4 Results

The stress–strain relationship was approximately linear in spinal cord specimens without the pia mater. In contrast, this relationship was nonlinear in specimens containing the pia mater, demonstrating a concave upward curve similar to that commonly observed in connective tissue (Fig. 6.4).

The elastic moduli of spinal cords with and without the pia mater were 16 ± 5 and 5 ± 2 kPa, respectively. The presence of the pia mater increased the elastic modulus of the spinal cord threefold. The width of the spinal cord cross section was 5 ± 0.5 mm

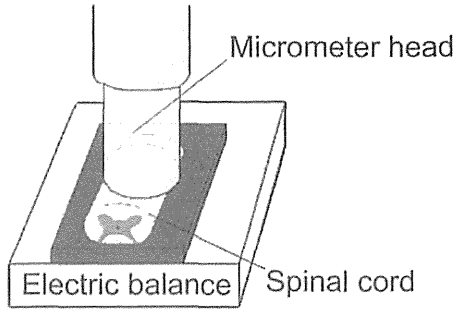

Fig. 6.5 Compression test of the spinal cord. A micrometer head compressed the specimen placed on an electric balance with a 50 μm increase at 60 s intervals. The load applied to the specimen was measured 30 s after every increase in compression

and the thickness of the pia mater was 12±3 μm (five specimens). The elastic modulus of the pia mater was calculated to be 2,300 kPa, which was 460 times greater than that of the spinal cord without the pia mater.

6.3.2 Compression Test of the Spinal Cord with an Intact or Incised Pia Mater Stiffness of the Spinal Cord

6.3.2.1 Materials and Methods

Four Japanese white rabbits were used in this test. The method of specimen preparation was the same as that used for the tensile test. Each spinal cord segment was divided into two pieces for the compression test. In one piece, the pia mater was kept intact, and in the other it was incised longitudinally at both sides while viewed with a microscope. Each specimen was transferred into a Petri dish filled with physiological saline solution, which was then placed on an electrical balance (model AEG-220; Shimadzu Corp., Kyoto, Japan). The specimen was compressed using a micrometer head (model MHK-25V; Mitutoyo Corp., Kanagawa, Japan) with a 50 μm increase in compression at 60 s intervals (Fig. 6.5). The original measurement was obtained at the point at which the micrometer head touched the surface of the specimen. The load applied to the specimen was measured 30 s after every increase in compression. Stiffness, a parameter indicating the amount of mechanical resistance against a unit deformation, was calculated as the ratio of the load increment to the 50 μm increase in compression.

Specimens were fixed in 10 % neutral buffered formalin after the compression test. They were then dehydrated and embedded in paraffin. Sections 5 μm thick were obtained and stained with H&E. The morphological characteristics of the specimens were observed.

6.3.2.2 Results

There was no significant difference in stiffness between specimens with an intact pia mater and those with an incised pia at a compression less than 1 mm.

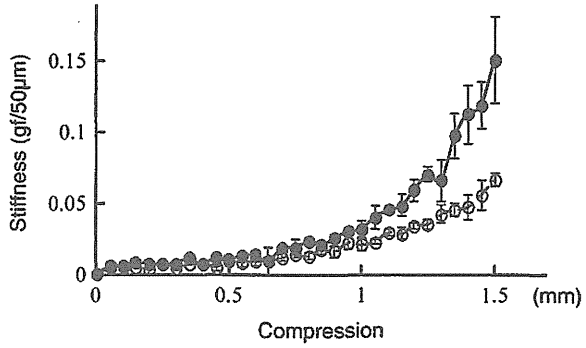

Fig. 6.6 The stiffness is shown as the ratio of the load increment to the increase of 50 μm deformation. No significant difference between the stiffness of specimens with the intact and incised pia mater was found at compression less than 1.00 mm. With an increase in the compression over 1.00 mm, the stiffness of the specimen with the intact pia mater increased significantly more than that of the one with the incised pia mater ($p<0.05$) (*open circle*, spinal cord with incised pia; *filled circle*, spinal cord with intact pia; mean ± SD)

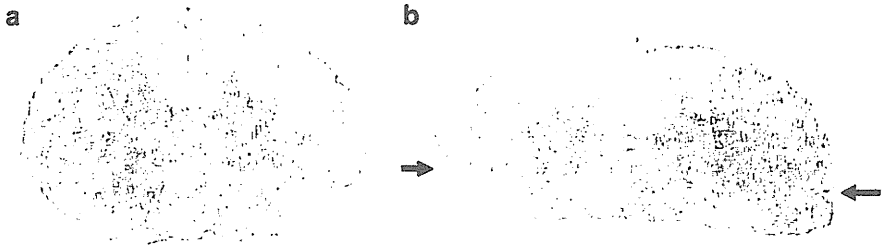

Fig. 6.7 The shape of the specimen with the intact pia mater was well restored after the removal of the compression on H&E-stained section (a), while the specimen with the incised pia mater remained in a deformed state (b). *Arrows* indicate places where the pia mater was cut at both sides of the specimen (×10)

At a compression greater than 1 mm, however, the stiffness of the specimen with the intact pia mater increased significantly more than the one with the incised pia mater ($p<0.05$) (Fig. 6.6).

A histological investigation revealed that the shapes of specimens with an intact pia mater were well restored after removal of the compression. In contrast, specimens with an incised pia mater remained deformed (Fig. 6.7).

6.3.3 Discussion

Our results demonstrated the following. The pia mater had an elastic modulus of 2,300 kPa, which was 460 times greater than that of the spinal cord parenchyma. By covering the parenchyma, it tripled the elastic modulus of the spinal cord as a whole.

The pia mater increased the stiffness of the spinal cord and enhanced its recovery of shape after removal of the compression.

Spinal pia mater consists of two layers: the intima pia (inner layer) and the epipial tissue (outer layer). The inner layer is a network of fine elastic fibers closely attached to spinal cord parenchyma. The outer layer is relatively thick and formed by a loose mesh of collagen fiber bundles that partially extends into the arachnoid trabeculae [10]. The elastic moduli of elastic and collagen fibers have been reported to be approximately 600 kPa and 1,000 MPa, respectively [11]. Accordingly, the elastic modulus of the pia mater, which measured 2,300 kPa in the present study, seems to depend mainly on the elasticity of the elastic fibers and partly on that of the collagen fibers.

Stiffness indicates the inflexibility of the spinal cord against compression; this is expressed as the ratio of the increment of the load to an increase in compression. When tissue is resistant to deformation, which is referred to as high stiffness, the load sharply increases as the compression increases. On the other hand, when tissue is easily deformed, referred to as low stiffness, the load gradually increases. The results of the present study verified that spinal cord containing an intact pia mater had greater stiffness. Thus, the pia mater is rigid enough to increase the overall stiffness of the spinal cord.

After the compression test, the shape of the spinal cord with an intact pia mater was well restored; however, the shape of the spinal cord with an incised pia mater scarcely recovered. This indicates that, as a result of being tightly covered by the pia mater, the compressed spinal cord contains a large amount of strain energy, which enables shape restoration after decompression.

6.4 Effect of the Tensile Stress on the Morphology of the Spinal Cord

The spinal cord is physiologically stretched along the craniocaudal axis and is subjected to tensile stress. Breig and el-Nadi [12] reported that the spinal canal decreases in length when the spine is extended and increases in length when the spine is flexed in human cadavers. The spinal cord adapts to these changes of length by elongating and shortening itself. Tensile stress in the spinal cord is produced by the stretching of the spinal cord.

In cervical myelopathy, the spinal cord is deformed according to compression as observed on CT myelograms and axial MR images. The cross-sectional area of the spinal cord decreases in response to compression and increases after surgery [13]. Although various mechanical factors regulating the morphology of the spinal cord have been studied, the influence of physiological tensile stress in the spinal cord has not been studied from the viewpoint of the morphological plasticity. The purpose of this study was to investigate the effect of the tensile stress on the morphology of the spinal cord under compression and decompression in rabbits.

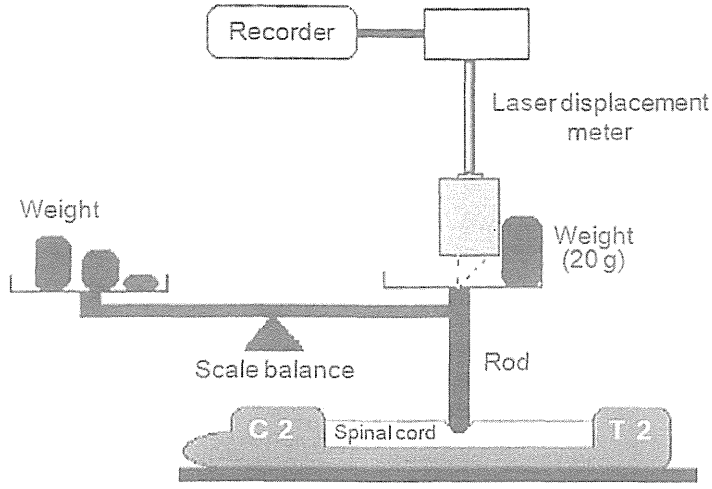

Fig. 6.8 Schematic drawing of the indentation test of the spinal cord. A rod of 5 mm in diameter was placed on the spinal cord. The rod was connected with a pan of a scale balance. Varying the weight on the other scalepan, the indentation of the rod on the spinal cord was measured with a laser displacement meter as a vertical displacement of the pan

6.4.1 *Materials and Methods*

Four Japanese rabbits were killed by intravenous injection of a high-dose pentobarbital. The spinal column and cord from C1 to T2 were excised from each rabbit. The specimens were maintained moist with a physiological saline solution during testing. Room temperature was kept at 18 °C.

All tests were accomplished within 40 min after the excision. The laminae and lateral masses between C3 and C7 were removed, and the specimen was put on the flat test table with the vertebral body down. After removal of the posterior half of the dura mater and the arachnoid membrane, the dentate ligaments and anterior and posterior rootlets were carefully dissected between C3 and C7. It was confirmed that the spinal cord on the spinal column did not adhere to the surrounding structure. A rod of 5 mm in diameter was placed on the midline of the spinal cord. The rod was connected with a pan of a scale balance (Fig. 6.8). Varying the weight on the other scalepan, the indentation of the rod on the spinal cord was measured as a vertical displacement of the pan using a laser displacement meter (LD-1100S-005, Ono Sokki, Tokyo, Japan) at C3/4 and C5 levels (2 points). The origin of the measurement was taken as the point before applying the load. The load on the spinal cord was increased from 0 to 1, 3, 5, 10, and 20 g and then decreased to 10, 5, 3, 1, and 0 g at 60 s intervals. The displacement was measured just before the load change. Then, the spinal cord was cut transversely and separated at C2/3 and C7/T1, and the

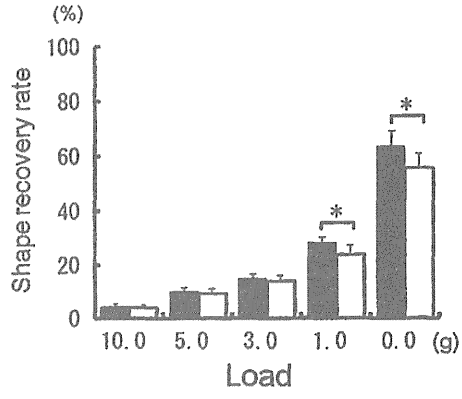

Fig. 6.9 Shape recovery rate after the separation (*shaded bar*) was significantly lower than that before the separation (*black bar*) at both 1 and 0 g ($n=8$, mean ± SD, $^*p<0.05$)

longitudinal tensile stress was removed. The samples were measured again with the same protocol at 2 points 10 mm caudal to each premeasured point on the spinal cord so that the residual indentation of the spinal cord caused by the previous measurement did not affect the new measurement. The shape recovery rate was defined as the proportion of elastic recovery under unloaded condition to the maximum deformation as follows: a shape recovery rate (%) = (maximum indentation − residual indentation)/maximum indentation × 100.

The shape recovery rate of 100 % indicated a complete recovery to the original condition.

6.4.2 *Results*

The craniocaudal length of the spinal cord between C2/3 and C7/T1 was 55.5 ± 3.9 mm before the separation and 50.1 ± 3.8 mm after the separation. The spinal cord was shortened by 9.7 % after the separation ($p<0.01$).

The recovery rate was not significantly different between the separated and unseparated cords until 3 g (Fig. 6.9). At the load of 1 g, the recovery rate was 28.0 ± 2.2 % before the separation and 23.6 ± 3.5 % after the separation. At the load of 0 g, the recovery rate was 63.1 ± 5.9 % before the separation and 55.5 ± 5.3 % after the separation. The recovery rate after the separation was significantly lower than that before the separation at both 1 and 0 g ($p<0.05$).

6.4.3 *Discussion*

Reid [14] described that the length of the spinal dura mater and spinal cord was increased in flexion and that the average stretching between C2 and C5 was approximately 10 %. Kuwazawa et al. [15] reported that the mean elongation of the length

of the cervical cord from extension to flexion was 11.7 mm in recumbent volunteers and 9.5 mm in erect volunteers on T2WI sagittal MR images. These values corresponded to 10.9 % and 8.9 % of the length in the extension position, respectively. In the present study, the spinal cord was placed in the straight position, and it was shortened by 10 % after the separation. This value was in agreement with the aforementioned studies.

We described the factors causing shape recoverability of the spinal cord after decompression in cervical myelopathy [16]. Shape recovery at an early stage after decompression may result from the movement of interstitial fluid from the periphery of the compressed site to the decompressed site. The spinal cord parenchyma exhibited viscoelasticity and an extremely low limit of elasticity [17]. This indicates that the shape recovery of the spinal cord after decompression cannot occur by itself. The shape recovery must thus be induced by the strain energy in the spinal cord, that is, the intramedullary pressure [18]. Iida and Tachibana [19] demonstrated that the spinal cord intramedullary pressure is increased by mechanical compression on the anterior structure of the spinal canal and stretching of the cord in canine studies. Therefore, the tensile stress in the spinal cord can increase the intramedullary pressure and enhance the shape recoverability of the spinal cord [20].

Conflict of Interest The authors declare that they have no conflict of interest.

References

1. Levine DN (1997) Pathogenesis of cervical spondylotic myelopathy. J Neurol Neurosurg Psychiatry 62:334–340
2. Ohashi T, Matsumoto T, Abe H et al (1997) Intramural distribution of local elastic moduli in bovine thoracic aorta measured by pipette aspiration method. Cellular Eng 2:12–18
3. Aoki T, Ohashi T, Matsumoto T et al (1997) The pipette aspiration applied to the local stiffness measurement of soft tissue. Ann Biomed Eng 25:581–587
4. Evans EA (1973) New membrane concept applied to the analysis of fluid shear and micropipette-deformed red cells. Biophys J 13:941–954
5. Sato M, Levesque MJ, Nerem RM (1987) An application of the micropipette technique to the measurement of the mechanical properties of cultured bovine aortic endothelial cells. J Biomech Eng 109:27–34
6. Kokubun S, Tanaka Y (1995) Type of cervical disc herniation and relation to myelopathy and radiculopathy. J Back Musculoskelet Rehabil 5:145–154
7. Panjabi MM, White AAIII (1988) Biomechanics of nonacute cervical spinal cord trauma. Spine 13:838–842
8. Breig A (1960) Biomechanics of the central nervous system: some basic normal and pathologic phenomena. Year Book Publishing, Chicago
9. Tunturi AR (1978) Elasticity of the spinal cord, pia, and denticulate ligament in the dog. J Neurosurg 48:975–979
10. Millen JW, Woollam DHM (1961) On the nature of the pia mater. Brain 84:514–520
11. Fung YC (1993) Biomechanics: mechanical properties of living tissues, 2nd edn. Springer, New York
12. Breig A, el-Nadi AF (1966) Biomechanics of the cervical spinal cord. Relief of contact pressure on and overstretching of the spinal cord. Acta Radiol Diagn 4:602–624

13. Ozawa H, Matsumoto T, Ohashi T et al (2004) Mechanical properties and function of the spinal pia mater. J Neurosurg Spine 1:122–127
14. Reid JD (1960) Effects of flexion-extension movements of the head and spine upon the spinal cord and nerve roots. J Neurol Neurosurg Psychiatry 23:214–221
15. Kuwazawa Y, Pope MH, Bashir W et al (2006) The length of the cervical cord: effects of postural changes in healthy volunteers using positional magnetic resonance imaging. Spine 31:E579–583
16. Bilston LE, Thibault LE (1996) The mechanical properties of the human cervical spinal cord in vitro. Ann Biomed Eng 24:67–74
17. Ozawa H, Matsumoto T, Ohashi T et al (2001) Comparison of spinal cord gray matter and white matter softness: measurement by pipette aspiration method. J Neurosurg 95(2 Suppl):221–224
18. Tachibana S, Kitahara Y, Iida H et al (1994) Spinal cord intramedullary pressure. A possible factor in syrinx growth. Spine 19:2174–2178
19. Iida H, Tachibana S (1995) Spinal cord intramedullary pressure: direct cord traction test. Neurol Med Chir (Tokyo) 35:75–77
20. Ozawa H, Matsumoto T, Ohashi T et al (2011) Stretch along the craniocaudal axis improves shape recoverability of the spinal cord. J Biomech 44:2313–2315

Chapter 8
Morphologic Change and Glial Response to Unilateral Spinal Cord Compression

Hiroshi Ozawa and Jianwu Zhao

Abstract In cervical myelopathy, unilateral compression of the spinal cord would be expected to produce Brown-Séquard syndrome. However, transverse lesion syndrome occurs in most clinical cases. In order to reveal the mechanism by which unilateral compression induces transverse damage to the spinal cord, damage of the gray and white matter in each half of the spinal cord was examined precisely using the density of reactive glial cells. The cervical spinal cord in rabbits was unilaterally compressed with a small screw. The area of each half of the damaged cord and the densities of GFAP-positive astrocytes and reactive microglias of the compressed and contralateral halves were investigated. As the compression increased, the area of the compressed half of the spinal cord decreased significantly compared to the contralateral half. The densities of GFAP-positive astrocytes in the gray matter and the anterior funiculus significantly increased in the compressed half. There were no significant differences in the densities at the lateral and dorsal funiculi between the compressed and contralateral halves. The tissue damage in the gray matter of the compressed half was markedly higher. These findings provide evidence for the mechanistic basis of spinal cord damage that leads to transverse lesion syndrome in unilateral compression myelopathy.

Keywords Astrocyte • Microglia • Transverse lesion syndrome • Unilateral spinal cord compression

H. Ozawa (✉)
Department of Orthopaedic Surgery, Tohoku University School of Medicine,
1-1 Seiryomachi, Aobaku, Sendai 980-8574, Japan
e-mail: hozawa@med.tohoku.ac.jp

J. Zhao
Department of Orthopaedics, Chian-Japan Union Hospital,
Jilin University, Changchun 130033, China

K. Uchida et al. (eds.), *Neuroprotection and Regeneration of the Spinal Cord*,
DOI 10.1007/978-4-431-54502-6_8, © Springer Japan 2014

8.1 Introduction

In cervical myelopathy due to chronic compression, the spinal cord is compressed either locally in cases of spondylosis and disc herniation or over its entire width in the cases of ossification of the posterior longitudinal ligament (OPLL) and spinal canal stenosis. The former type of compression is classified into median and unilateral compression [1–3]. Theoretically, unilateral compression of the spinal cord should produce a Brown-Séquard syndrome consisting of ipsilateral motor dysfunction and contralateral sensory disturbances below the level of the lesion. However, it clinically produces transverse lesion syndrome consisting of bilateral motor and sensory deficits of the lower limbs with almost equal severity in most cases [4–7]. This suggests that the unilateral compression exerts some mechanical effects on the contralateral side of the spinal cord as well as the compressed side.

The pathomechanisms of spinal cord injury and myelopathy have been investigated. Numerous pathophysiologies of myelopathy resulting from either compression of the entire width or the median compression of the spinal cord have been reported [8–10]. In these experiments, however, the full width of the spinal cord was compressed or, if locally compressed, the compression site was not controlled. There have been no models reported in which the spinal cord is compressed unilaterally with control of the site and severity. Further the pathophysiology of the contralateral side compared to the compressed side has not been described in a unilateral compression model [11].

In order to reveal the mechanism by which the unilateral compression induced the transverse damage to the spinal cord, damage of the gray and white matter in each half of the spinal cord was examined via quantitative assessment of the glial cells.

8.2 Materials and Methods

8.2.1 Spinal Cord Compression Model

The experiments were conducted on Japanese white rabbits weighing approximately 3,000 g (range 2,800–3,200 g). The rabbits were anesthetized with intravenous pentobarbiturate (25 mg/kg). Following exposure of the anterior aspect of C5 body, the body was perforated to the epidural space using a high-speed drill (2 mm in diameter) under a microscope. The hole was localized 2 mm to the right of the midline. A screw (2.1 mm in diameter) with a round tip was gradually driven through the hole to compress the spinal cord. For the appropriate evaluation of the proliferating glial cells, the screw was placed to protrude 2 mm into the spinal canal as mild compression and 3 mm as moderate compression. Three rabbits served as sham controls. They were examined for motor functions using Tarlov's rate of functional recovery [12] the next day and 1 week after the surgery.